ELSEVIER

European Journal of Pharmacology 373 (1999) 251–262

ejp

www.elsevier.nl/locate/ejphar

Characterization of a new AMPA receptor radioligand, [^{3}H]2-amino-3-(3-carboxy-5-methyl-4-isoxazolyl)propionic acid

Tine B. Stensbøl [a], Frank A. Sløk [a], Joseph Trometer [b], Stephen Hurt [b], Bjarke Ebert [c], Connie Kjøller [d], Jan Egebjerg [e], Ulf Madsen [a], Nils H. Diemer [d], Povl Krogsgaard-Larsen [a,*]

[a] *PharmaBiotec Research Center, Department of Medicinal Chemistry, The Royal Danish School of Pharmacy, 2 Universitetsparken, DK-2100 Copenhagen, Denmark*

[b] *Medical Products Department, E.I. Du Pont De Nemours, Boston, MA, USA*

[c] *PharmaBiotec Research Center, Department of Pharmacology, The Royal Danish School of Pharmacy, Copenhagen, Denmark*

[d] *Institute of Neuropathology, University of Copenhagen, Copenhagen, Denmark*

[e] *Department of Molecular and Structural Biology, University of Aarhus, Aarhus, Denmark*

Received 7 April 1999; accepted 13 April 1999

Abstract

(*RS*)-2-Amino-3-(3-carboxy-5-methyl-4-isoxazolyl)propionic acid (ACPA), which is a potent and selective agonist at (*RS*)-2-amino-3-(3-hydroxy-5-methyl-4-isoxazolyl)propionic acid (AMPA) receptors, has previously been shown to desensitize AMPA receptors to a much lower degree than AMPA itself. We now report the synthesis of [^{3}H]ACPA (32.5 Ci/mmol), the neurochemical and pharmacological characterization of [^{3}H]ACPA binding, and a comparison of the distribution of [^{3}H]ACPA, [^{3}H]AMPA, and [^{3}H](*S*)-5-fluorowillardiine binding sites in rat brain. Under equilibrium conditions, [^{3}H]ACPA was shown to bind to a single population of receptor sites on rat brain membranes. [^{3}H]ACPA was shown to bind with single and similar affinities (15–45 nM) to cloned AMPA receptor subunits (GluR1–4), expressed in insect cells, whereas a K_D value of 330 nM was determined for the binding of [^{3}H]ACPA to cloned kainic acid preferring GluR5 subunits. Whereas B_{max} and K_D values for [^{3}H]ACPA binding, determined using filtration techniques, were different from such obtained in centrifugation assays, B_{max} and K_D values as well as association and dissociation constants were not significantly affected by the addition of the chaotropic agent KSCN. K_D values, determined under equilibrium conditions, were, however, markedly different from K_D values derived from kinetic data. Furthermore, the results of analyses of these kinetic data were consistent with the existence of two different populations of [^{3}H]ACPA binding sites. The pharmacology of [^{3}H]ACPA binding sites was characterized using a series of AMPA receptor agonists and antagonists. Whereas addition of KSCN had little effect on the affinities of AMPA receptor agonists for [^{3}H]ACPA binding, this chaotropic agent reduced the affinities of AMPA receptor antagonists structurally related to AMPA. Based on these and previously reported data, the AMPA receptor agonists, ACPA, AMPA and (*S*)-5-fluorowillardiine, seem to bind to and activate AMPA receptors in a nonidentical fashion, and these three agonists together may be useful tools for studies of AMPA receptor mechanisms.

Keywords: AMPA receptor; ACPA ((*RS*)-2-Amino-3-(3-carboxy-5-methyl-4-isoxazolyl)propionic acid); Receptor autoradiography; Thiocyanate

1. Introduction

(*S*)-Glutamic acid ((*S*)-Glu) is considered to be the major excitatory amino acid in the mammalian central nervous system. (*S*)-Glu receptors are divided into ligand-gated ionotropic receptors and G-protein coupled metabotropic receptors. The ionotropic receptors are furthermore subdivided into *N*-methyl-D-aspartate (NMDA), (*RS*)-2-amino-3-(3-hydroxy-5-methyl-4-isoxazolyl)propionic acid (AMPA) and kainic acid receptors (Krogsgaard-Larsen and Hansen, 1992; Collingridge and Watkins, 1994; Wheal and Thomson, 1995; Monaghan and Wenthold, 1997). Binding of [^{3}H]AMPA to rat cortical membranes has previously been shown to consist of two components, one component displaying high affinity for AMPA receptors with a K_D of 14 nM, and another component displaying low affinity with a K_D of 235 nM (Honoré and Drejer, 1988). The binding of the enantiomer [^{3}H](*S*)-AMPA is described to be twice as potent as the racemate

* Corresponding author. Tel.: +45-35370850 Ext. 247; Fax: +45-35372209; E-mail: nordly@medchem.dfh.dk

0014-2999/99/$ - see front matter
PII: S0014-2999(99)00269-1

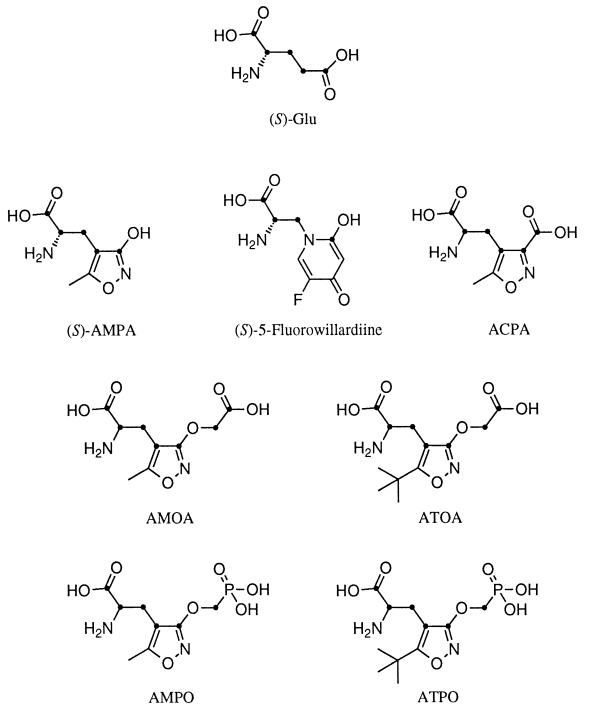

Fig. 1. Structures of (*S*)-Glu and a number of AMPA receptor agonists and antagonists.

(Hawkins et al., 1995b; Hawkinson and Espitia, 1997). The selective AMPA receptor agonist [^{3}H](*S*)-5-fluorowillardiine also binds to a high affinity and a low affinity component of AMPA receptors, but in contrast to what has been shown for the binding of [^{3}H](*S*)-AMPA, the affinity of [^{3}H](*S*)-5-fluorowillardiine is independent of the presence of the chaotropic agent KSCN (Hawkins et al., 1995a).

(*RS*)-2-Amino-3-(3-carboxy-5-methyl-4-isoxazolyl)propionic acid (ACPA) has previously been found to be a selective AMPA receptor agonist, more potent than AMPA itself (Madsen and Wong, 1992). In studies using recombinant GluR1 flop receptors expressed in *Xenopus* oocytes, ACPA was shown to be five times more potent than AMPA (Wahl et al., 1996). Furthermore, the maximum response elicited by ACPA turned out to be approximately four-fold higher than that elicited by AMPA, suggesting that ACPA desensitizes the AMPA receptor to a level markedly different from that observed for AMPA. These observations in conjunction with the results of binding studies (Hawkins et al., 1995a) may indicate that ACPA, which is a homologue of (*S*)-Glu, interacts with the recognition site of the AMPA receptor in a manner different from that of the (*S*)-Glu analogues, AMPA and (*S*)-5-fluorowillardiine (Fig. 1).

We here report the synthesis and subsequently the characterization of the binding of [^{3}H]ACPA in rat brain homogenates, in cell lines expressing ionotropic GluR1–4 and GluR5–6 receptors and in quantitative autoradiography using rat brains.

2. Materials and methods

2.1. Radiolabelling

The synthesis of [^{3}H]ACPA was based on a reaction sequence analogous with that developed for the preparation of [^{2}H]ACPA as outlined in Fig. 2. The synthesis of the starting material, methyl 2-acetamido-2-methoxycarbonyl-3-[5-(dibromomethyl)-3-methoxycarbonyl-4-isoxazolyl]propionate (**1**) will be reported elsewhere (F.A. Sløk, to be published).

*2.1.1. Methyl 2-acetamido-2-methoxycarbonyl-3-[5-(dideuteriomethyl)-3-methoxycarbonyl-4-isoxazolyl]propionate (**2**)*

To a solution of **1** (50 mg; 0.1 mmol) in tetradeuteriomethanol ($C^2H_3O^2H$; 0.5 ml) was added Pd/C (15 mg; 5%), and the reaction flask was closed with a rubber septum. To this suspension was added a stream of deuterium ($^2H_2$) for a period of 20 min. The reaction mixture was filtered, and to the filtrate were added dichloromethane (5 ml) and water (2 ml). The organic phase was dried ($MgSO_4$), filtered, and evaporated, and the residue was subjected to column chromatography on silica gel (gradient elution consisting of ethyl acetate:toluene (1:1)–(3:1)). Yield of **2**: 29 mg (84%). ^{1}H Nuclear Magnetic Resonance (NMR) (deuteriochloroform, tetramethylsilane): δ 6.67 (1H, s, NH), 3.93 (3H, s, OCH_3), 3.79 (6H, s, $2 \times OCH_3$), 3.65 (2H, s, CH_2), 2.34 (1H, m, CH^2H_2), 1.98 (3H, s, CH_3CO). ^{13}C NMR (deuteriochloroform): δ 171.0, 169.3, 167.9, 161.0, 154.3, 109.1 (C4), 65.3, 53.4 ($2 \times OCH_3$), 52.4 (OCH_3), 25.6 (CH_2), 22.6 (CH_3CO), 10.4 (CH^2H_2).

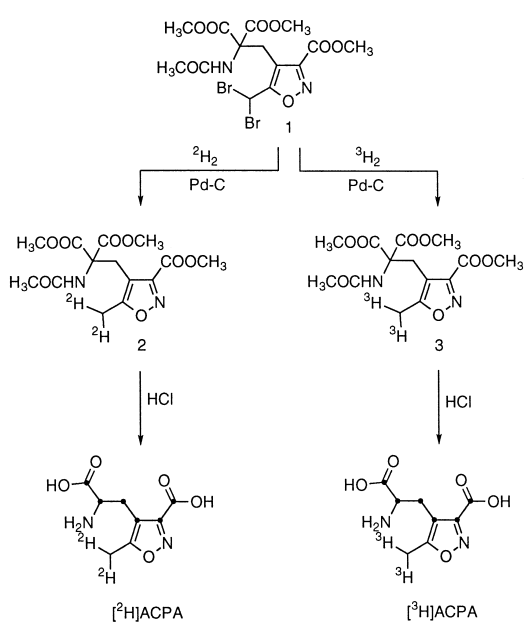

Fig. 2. Synthesis of [^{3}H]ACPA, based on model experiments for the synthesis of [^{2}H]ACPA.

The structural assignment was supported by ^{13}C-DEPT-135 and ^{13}C-GATEDEC NMR spectroscopy.

2.1.2. (RS)-2-Amino-3-[3-carboxy-5-(dideuteriomethyl)-4-isoxazolyl]propionic acid ([^{2}H]ACPA).

A solution of **2** (25 mg; 0.075 mmol) in hydrochloric acid (1 M; 5 ml) was refluxed for 12 h. Evaporation to dryness and addition of water (5 ml) and reevaporation three times gave [^{2}H]ACPA as a viscous oil (16 mg; ca. 50%). ^{1}H NMR (deuteriumoxide, dioxane): δ 4.14 (1H, t, J = 6.2 Hz, CH), 3.29 (1H, dd, J = 15 and 6.2 Hz, CHH), 3.17 (1H, dd, J = 15 and 6.2 Hz, CHH), 2.43 (1.3 H, m, CH^2H$_2$ and CH_2^2H). ^{13}C NMR (deuteriumoxide, dioxane): δ 172.7, 171.7, 163.3, 155.6, 110.2 (C4), 53.3 (CH), 24.1 (CH_2), 11.0 (CH^2H_2).

*2.1.3. Methyl 2-acetamido-2-methoxycarbonyl-3-[5-(ditritiomethyl)-3-methoxycarbonyl-4-isoxazolyl]propionate (**3**)*

Compound **1** (23 mg; 0.045 mmol) was dissolved in methanol (0.5 ml) and triethylamine (0.025 ml) in a 5 ml tritiation flask. To the reaction mixture was added Pd/C (15 mg; 5%), and the flask was charged with tritium ($^3H_2$) gas. The reaction was stirred at 25°C and atmospheric pressure for 2 h. Labile $^3H_2$ was removed with ethanol and the crude material was assayed to afford 240 mCi. The crude reaction mixture was purified by high performance liquid chromatography (HPLC) on a Zorbax RX-C8 semipreparative column with a mobile phase of 1% triethylammonium acetate (pH 4)/acetonitrile (55:45) at a flow rate of 2 ml/min. The material corresponding to **2** (detected by UV absorbance at 254 nm) had a retention time of ca. 18 min. The mobile phase was removed under reduced pressure with multiple ethanol azeotropic evaporations. The residue was taken up into ethanol (10 ml) and assayed to give 135 mCi. The specific activity of **3** was 32.5 Ci/mmol as determined by mass spectrometry (DCI).

2.1.4. (RS)-2-Amino-3-[3-carboxy-5-(ditritiomethyl)-4-isoxazolyl]propionic acid ([^{3}H]ACPA)

Compound **3** (135 mCi; 13.5 mCi/ml; 32.5 Ci/mmol) was dissolved in ethanol (5 ml) in a 25 ml round bottom flask. The solvent was removed under reduced pressure, and the residue was taken up into hydrochloric acid (1 M; 5 ml). This mixture was refluxed for 20 h under argon. The crude reaction mixture was purified by HPLC on a Zorbax RX-C8 semipreparative column with a mobile phase of 1% triethylammonium acetate (pH 4) at a flow rate of 2 ml/min. The material corresponding to [^{2}H]ACPA (detected by UV absorbance at 254 nm) had a retention time of ca. 14 min. The mobile phase was removed under reduced pressure with multiple ethanol azeotropic evaporations. The residue was taken up into water–ethanol (1:1; 20 ml) solution and assayed to give 85 mCi. The purity of [^{3}H]ACPA was found to be 99% when checked by HPLC on a Zorbax RX-C8 analytical column with a mobile phase of 1% triethylammonium acetate (pH 4). [^{3}H]ACPA was obtained with a specific radioactivity of 32.5 Ci/mmol.

2.2. Materials

[^{3}H]ACPA (32.5 Ci/mmol) was synthesized as described above. [^{3}H]AMPA (53.1 Ci/mmol) and [^{3}H](*S*)-5-fluorowillardiine (45.0 Ci/mmol) were obtained from Dupont NEN Products (Boston, MA, USA). 2,3-Dihydroxy-6-nitro-7-sulfamoylbenzo[*f*]quinoxaline (NBQX) was a gift from NeuroSearch, Glostrup, Denmark. The following compounds were synthesized according to published procedures: AMPA (Begtrup and Sløk, 1993); ACPA (Madsen and Wong, 1992); (*RS*)-2-amino-2-(5-*tert*-butyl-3-hydroxy-4-isoxazolyl)propionic acid (ATPA) (Lauridsen et al., 1985); (*RS*)-2-amino-3-(3-carboxymethoxy-5-methyl-4-isoxazolyl)propionic acid (AMOA) (Krogsgaard-Larsen et al., 1992); (*RS*)-2-amino-3-(5-*tert*-butyl-3-carboxymethoxy-4-isoxazolyl)propionic acid (ATOA), (*RS*)-2-amino-3-(5-methyl-3-phosphonomethoxy-4-isoxazolyl)propionic acid (AMPO), and (*RS*)-2-amino-3-(5-*tert*-butyl-3-phosphonomethoxy-4-isoxazolyl) ropionic acid (ATPO) (Madsen et al., 1996). All other chemicals were obtained through standard commercial sources.

2.3. Rat brain membrane preparation

Male Sprague Dawley rats (200–250 g) were decapitated and forebrain tissue consisting of cerebral cortex, striatum and hippocampus was quickly removed and homogenized in 15 volumes of ice-cold 30 mM Tris–HCl buffer containing 2.5 mM $CaCl_2$ (pH 7.4). The homogenate was centrifuged at 30 000 × g for 15 min and the resulting membrane pellet was washed three times by resuspension in approximately 15 volumes of buffer, each time followed by centrifugation. The pellet, resuspended in buffer, was incubated at 37°C for 30 min, centrifuged (30 000 × g, 15 min) and then washed and centrifuged three more times. The final pellet was resuspended in approximately 10 volumes of buffer and frozen at 18°C for up to 6 months prior to the assay. On the day of the experiment, frozen homogenates were thawed and resuspended in 50 volumes of ice-cold buffer (30 mM Tris–HCl, 2.5 mM $CaCl_2$, pH 7.4) and centrifuged (30 000 × g, 10 min). This step was repeated four times. In experiments using chaotropic conditions, 100 mM KSCN was added to the buffer during the washing step and during incubation. The final pellet was resuspended in ice-cold buffer corresponding to approximately 40 mg original tissue per ml. Assays were carried out in a final volume of 250 μl consisting of 25 μl [^{3}H]ACPA, 25 μl test solution, and 200 μl membrane suspension, corresponding to approximately 8 mg original tissue per aliquot. All assays were

carried out both as centrifugation and filtration assays with or without KSCN, unless otherwise stated.

2.4. Brain membrane binding experiments

Following incubation at 0–4°C for up to 90 min, filtration was carried out through GF/B filters using a 96-well Packard FilterMate Cell Harvester and washing three times with 250 μl ice-cold buffer (30 mM Tris–HCl, 2.5 mM $CaCl_2$, pH 7.4). Filters were dried and 25 μl Microscint 0 was added. The amount of [^{3}H]ACPA bound to the membranes was determined using a Packard TOPCOUNT, microplate scintillation counter with a counting efficiency of 25%. Data are means of three individual experiments run in triplicates.

Following incubation at 0–4°C for up to 90 min, centrifugation was carried out using a Sorvall FA-MICRO RMC-14 microcentrifuge (18 500 × *g*, 3 min) and washing with ice-cold (3 × 1 ml) buffer (30 mM Tris–HCl, 2.5 mM $CaCl_2$, pH 7.4). The pellets were solubilized in 100 μl 1% w/v sodium *n*-dodecylsulfate overnight and 1.0 ml of Opti-fluor was added. The amount of bound radioactivity was determined using a TRI-CARB liquid scintillation analyzer (model 2000 CA) with a counting efficiency of 56%. Data are means of three individual experiments run in duplicates.

For both centrifugation and filtration assays, nonspecific binding was determined in the presence of (*S*)-Glu (final concentration 1 mM) instead of test solution. Total binding was determined by adding water instead of test solution. All compounds were dissolved in water and all dilutions were made in water.

Saturation studies were carried using a method described by Morgan et al. (1991). Concentrations of [^{3}H]ACPA between 0.1 nM and 10 000 nM were used. Concentrations of radioligand between 0.1 and 50 nM were achieved by increasing the amount of labelled ligand, while those above 50 nM were achieved by isotope dilution of a fixed concentration of radioligand (50 nM).

Association studies were carried out by adding membrane suspension (200 μl) to [^{3}H]ACPA (25 μl) and water (25 μl) (total binding) or (*S*)-Glu (25 μl, final concentration 1 mM) (nonspecific binding). Nonspecific binding was determined initially, midway and at the end of the experiment.

Dissociation studies were carried out by incubating membrane suspension (200 μl) with [^{3}H]ACPA (25 μl) for 90 min. Dissociation was then initiated by adding (*S*)-Glu (25 μl, final concentration 1 mM) followed by a short vortex treatment. Total binding was determined initially, midway, and at the end of the experiment.

Experiments examining pH-dependence were only carried out by centrifugation. Membranes were incubated with buffer (30 mM Tris–HCl, 2.5 mM $CaCl_2$, 100 mM KSCN) with pH ranging from 5 to 8.5, and washed with the same buffer.

Inhibition experiments were carried out using 10 nM [^{3}H]ACPA and (*S*)-Glu, AMPA, ACPA, ATPA, quisqualic acid, kainic acid, AMOA, ATOA, AMPO, ATPO and NBQX as inhibitors.

2.5. Preparation of recombinant baculovirus

DNA fragments encoding the ionotropic (*S*)-Glu receptor subunits GluR1–GluR6 were generated by PCR employing primers, which eliminates the untranslated sequences and produced restriction sites facilitating the cloning in the transfer plasmid pFastBac (Life Technology). The DH10Bac (Life Technology) *Escherichia coli* strain carrying a bacmid was transformed with the pFastbac plasmids harbouring one of the GluR cDNAs, and recombinant bacmids were isolated and used for transfection of *S. frugiperda* (Sf21) insect cells. High Five (*Trichoplucia ni*, Invitrogen) cells were grown to 1–2 × 10^6 cells/ml and infected with recombinant virus at a multiplicity of 3. Cells were harvested by centrifugation 72 h after infection. The cell pellets were stored at −80°C.

2.6. Cell membrane preparation and binding assay

Binding was performed using crude membrane preparations made from the frozen cell pellets by homogenization (polytron) in AMPA binding buffer (30 mM Tris HCl pH 7.1, 2.5 mM $CaCl_2$) for GluR1–GluR4 or kainic acid binding buffer (5 mM HEPES–KOH, pH 7.1) for GluR5 and GluR6, and centrifuged (20 min). The crude pellet was washed three times in the respective binding buffers (supplemented with 0.2 mM phenylmethylsulfonylfluoride, 20 μg/ml aprotenin, 20 μg/ml benzamidine and 20 μg/ml iodoacetamide) by re-homogenization and centrifugation. The final pellet was either frozen for further use or re-dissolved in the respective binding buffers (supplemented with 100 mM KSCN for the GluR1-GluR4 containing cell membranes) for immediate use. Binding experiments were performed by incubating the samples (50–150 μg protein) with [^{3}H]ACPA for 90–120 min at 4°C. (*S*)-Glu (2 mM) was used to determine the nonspecific binding. Binding was terminated by rapid filtration through GF/C filters followed by three washes with ice-cold binding buffer.

2.7. Receptor autoradiography

Following a modified version of the method described by Nielsen et al. (1988) receptor autoradiography was carried out. Six adult male Wistar rats (250–300 g) housed on a 12 h light–dark cycle with free access to food and water were decapitated under 3% halothane anesthesia, the brains were quickly removed and frozen in isopentane/acetone at −80°C. From each animal, 40 horizontal 20 μm thick cryosections were cut at −16°C and thaw-mounted onto ethanol/hydrochloric acid/acetone cleaned cover-slips. The sections were stored at −80°C until fur-

ther processing. Adjacent sections were stained with hematoxylin–eosin for histopathologic examination.

On the day of the experiment, all sections were thawed for 15 min at 4°C prior to a 20 min preincubation at 4°C in 30 mM Tris–HCl buffer containing 2.5 mM $CaCl_2$ (pH 7.4) and 20 nM of each one of the three [^{3}H]labelled ligands used (AMPA, (*S*)-5-fluorowillardiine and ACPA). The incubation procedures for each of the three ligands were the same. For every three sections incubated, 100 mM KSCN and [^{3}H]labelled ligand were added to the buffer. Nonspecific binding was defined in the presence of 1 mM (*S*)-Glu for sections incubated both in the presence and absence of KSCN.

From each animal two sections were incubated in each ligand incubation solution. Radioligand not bound to the section was removed by three washes in ice-cold buffer, one wash in acetone/glutaraldehyde, and one final wash in ice-cold water (total duration of wash was 8 s). Following wash, the sections were dried under a stream of dry air.

Dried sections and [^{3}H]microscales were exposed to Amersham [^{3}H]Hyperfilm for three weeks. For each radioligand sections for all three incubation groups were exposed to the same [^{3}H]Hyperfilm. The radioligand concentrations in the incubation solutions were determined using liquid scintillation counting techniques. The optical densities were determined and transformed into nCi/mg tissue using a computer-aided image analysis system (Image 1.53 from NIH, USA) and the [^{3}H]microscales binding densities (fmol/mg tissue) of [^{3}H]ligand were calculated by correcting for specific activity of the radioligand in the incubation solution.

Statistical analysis was performed using Kruskal–Wallis one-way analysis of variance by rank with a significance level of 0.05.

2.8. Data analysis

Data were analyzed by the nonlinear curve fitting program GRAFIT 3.0 (Leatherbarrow, 1992). Data obtained from saturation, association and dissociation experiments were analyzed using equations describing one and two receptor binding sites. An *F*-test was used to determine whether equations describing two individual receptor binding sites fitted the data better than equations describing one binding site. $P < 0.05$ was used as significance level.

K_D values were calculated using the equation Bound = $(B_{max} \times [L])/(K_D + [L])$. Alternatively, K_D values were calculated by the equation described by Bennett and Yamamura (1985): $K_D = k_{-1}/k_{+1}$; $k_{+1} = (k_{obs} - K_{-1})/[L]$. Association data were fitted to the equation: $B_{max1}(1 - e^{-k_1 \times t}) + B_{max2} \times (1 - e^{-k_2 \times t})$. Dissociation data were fitted to the equation: $B_{max1} \times (1 - e^{-k_1 \times t}) + B_{max2} \times (1 - e^{-k_2 \times t})$. Inhibition data were fitted to the equation: Bound = $B_{max} \times (1 - [\text{Inhibitor}]/(IC_{50} + [\text{Inhibitor}])$. The K_i values were calculated using the method described by Cheng and Prusoff (1973): $K_i = IC_{50}/(1 + (L/K_D))$. *t*-Tests were used in order to elucidate differences in K_i values, and were carried out using pK_i values.

3. Results

3.1. Brain membrane binding: kinetics and pharmacology

Variations in specific binding caused by changes in the amount of original tissue, presence of $CaCl_2$ and KSCN were initially evaluated. As depicted in Fig. 3, the specific binding increased using from 2 to approximately 13 mg original tissue. A further increase in the amount of tissue used, did not result in a significant increase in the specific binding, due to the higher nonspecific binding. In order to ensure a high ratio between specific and nonspecific binding, samples of 8 mg tissue per aliquot were chosen for both filtration and centrifugation assays. In the presence of KSCN and at 7 nM [^{3}H]ACPA a total of 8000 dpm and a non-specific of 2000 dpm was observed using centrifugation assays, whereas a total of 5200 dpm and a nonspecific of 480 dpm was observed using filtration assays.

Addition of $CaCl_2$ did not significantly increase or decrease the specific binding (data not shown). However, in order to make the binding assay comparable to the assay for [^{3}H]AMPA binding, all of the remaining experiments were carried out in the presence of 2.5 mM $CaCl_2$.

Studies of the pH dependence (Fig. 4) disclosed small differences in the specific binding throughout the range of pH values examined, although a maximum at pH 7.5 could be seen. All of the remaining experiments were carried out at pH 7.4.

Using the conditions described above and filtration as the method of separation, specific binding of [^{3}H]ACPA to rat cortical membranes was determined to be 80% of the total counts in the absence of KSCN, and 86% in the presence of KSCN. In centrifugation assays, the specific binding was determined to be 71% in the absence of KSCN and 75% in the presence of KSCN, showing a

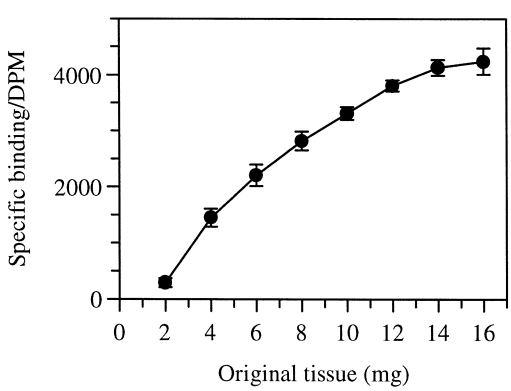

Fig. 3. Specific binding as a function of milligram original tissue. Values are mean values ± S.E.M. of three individual centrifugation experiments.

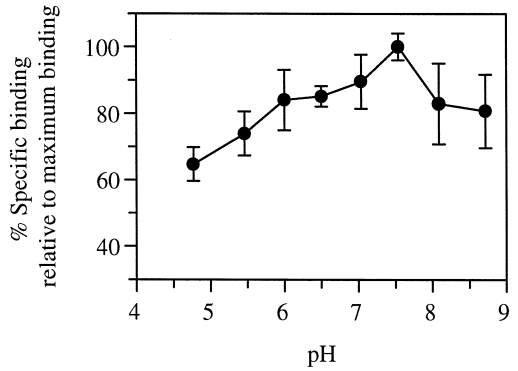

Fig. 4. The specific binding as a function of pH in the centrifugation assay. Values are mean values ± S.E.M. of four individual experiments.

higher proportion of nonspecific binding compared to filtration assays.

Results from the saturation experiments are shown in Table 1 and Fig. 5. Binding of [^{3}H]ACPA to rat cortical membranes was saturable in the presence and absence of KSCN. The K_D of [^{3}H]ACPA was found to be 260 ± 42 nM in the presence of KSCN and 430 ± 48 nM in the absence of KSCN, when filtration was used as the method to separate bound from free ligand. *F*-tests showed that equations assuming two independent receptor binding sites did not significantly improve curve fits to the data as compared to equations assuming only one binding site. The centrifugation assays also yielded data that were not fitted significantly better to equations assuming two different receptor populations as compared to one. The K_D values determined in the centrifugation assays, 920 ± 99 nM (+KSCN) and 1100 ± 390 nM (−KSCN), were significantly higher than those obtained using the filtration technique.

Association studies showed that the kinetics of association were best described by two exponential functions (Table 2 and Fig. 6), the largest receptor population occupying from 63 to 75% of the total number of binding sites, with rate constants ranging from 0.035 min^{-1} to 0.063

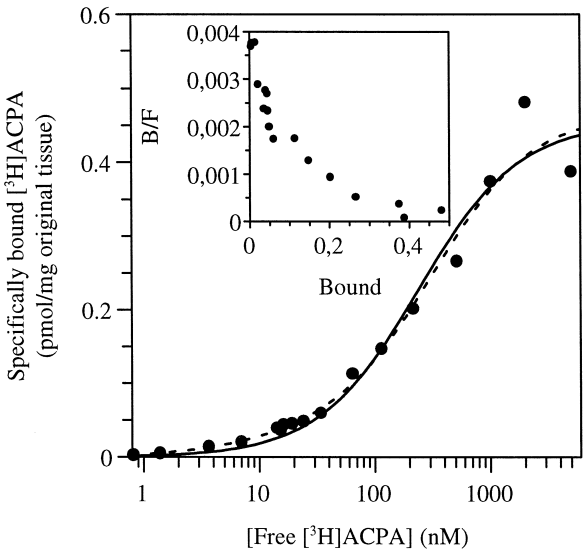

Fig. 5. Saturation curve and scatchard plot (inset) of [^{3}H]ACPA binding to rat cortical membranes in the presence of 100 mM KSCN. Data are from one experiment carried out by filtration, which was repeated three times with similar results. Full line shows a curve fit assuming one receptor population. Dashed line shows a curve fit assuming two independent receptor populations. Nonspecific binding was determined in the presence of 1 mM (*S*)-Glu.

min^{-1}, meaning that equilibrium was reached after 50–90 min of incubation. Displacement studies carried out with an incubation time of 60 or 90 min did not differ in the K_i values obtained (results not shown).

In agreement with these observations, dissociation studies (Table 3 and Fig. 6) showed that the kinetics of dissociation could best be described by two exponential functions, dividing the total population of receptor sites into two almost equal populations, one population dissociating fast and the other dissociating significantly slower. Calculations showed that after 1 min, 33% of the binding had dissociated in centrifugation assays whereas 11%/25% (+KSCN/−KSCN) had dissociated in filtration assays during the same timespan. The apparently faster dissocia-

Table 1
Affinities and densities for [^{3}H]ACPA binding to rat brain membranes

	K_D^a (nM)	K_D^b (nM)	B_{max} (pmol/mg original tissue)
Filtration			
+KSCN	260 ± 42	7.1	0.54 ± 0.06
−KSCN	430 ± 48	25	0.51 ± 0.09
Centrifugation			
+KSCN	920 ± 99	0.52	2.5 ± 0.2
−KSCN	1100 ± 390	1.5	1.5 ± 0.3

Values are mean ± S.E.M. of at least three individual experiments run in triplicates (filtration) or duplicates (centrifugation).
[a]Determined as equilibrium fitted to an equation assuming one receptor binding site as described in Section 2.
[b]Values calculated using the kinetically determined k_{+1} and k_{-1} mean values depicted in Table 2 and Table 3. Calculations were carried out as described in Section 2.

Table 2
Association of the specific binding of [^{3}H]ACPA to rat brain membranes

	+KSCN		−KSCN	
	Filtration	Centrifugation	Filtration	Centrifugation
B_{max1} (%)	75 ± 4	63 ± 3	69 ± 11	64 ± 9
$\alpha_{1\,obs}$ (min^{-1})	0.041 ± 0.012	0.063 ± 0.007	0.035 ± 0.013	0.064 ± 0.009
B_{max2} (%)	25 ± 6	27 ± 3	31 ± 11	36 ± 9.1
$\alpha_{2\,obs}$ (min^{-1})	3.4 ± 2.0	3.1 ± 0.9	0.71 ± 0.41	2.3 ± 1.9

Association constants and receptor densities.
Values are mean ± S.E.M. of three individual experiments run in triplicates (filtration) or duplicates (centrifugation).
Values were calculated from equations describing two exponential functions as described in Section 2.

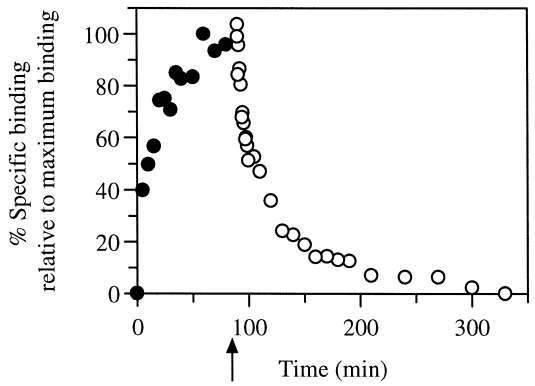

Fig. 6. Time course for the association (closed circles) and dissociation (open circles) of specific binding of 10 nM [^{3}H]ACPA to rat brain membranes. The data shown is from one experiment carried out as a filtration assay, which has been repeated twice with similar results. The arrow indicates start of dissociation, by addition of 25 μl (*S*)-Glu (final concentration 1 mM).

tion observed for the low affinity component of the [^{3}H]ACPA binding in centrifugation as compared to filtration may reflect that the time span between addition of (*S*)-Glu and termination of the reaction by centrifugation is not equal to the time, where the centrifugation is initiated. Thus, if the reaction is terminated at the end of the centrifugation and not as assumed at the start, this can explain the differences in dissociation rates.

The pharmacology of [^{3}H]ACPA binding was characterized in displacement studies, using a number of known agonists and antagonists. Results of these studies are summarized in Table 4. Correlation coefficients (r^2) for pK_i values obtained in centrifugation and filtration assays, were determined to be 0.982 and 0.968 in the presence or absence of KSCN, respectively.

When comparing pK_i values obtained in the presence or absence of KSCN, using the same method to separate bound from free ligand, differences in affinity were seen for some of the ligands (Fig. 7). Statistical analysis comparing pK_i values in the presence or in the absence of KSCN was carried out. The results showed that AMPA affinity was significantly enhanced in the presence of KSCN ($P < 0.05$ for centrifugation and $P < 0.001$ for filtration) resulting in an almost three-fold increase in affinity when KSCN was added to the buffer, whereas the affinity of (*S*)-Glu, ACPA, ATPA, kainic acid and quisqualic acid did not change significantly in the presence of KSCN (0.8–1.3 fold change in affinity) (Table 4). The

Table 3
Dissociation of the specific binding of [^{3}H]ACPA to rat brain membranes

	+KSCN		−KSCN	
	Filtration	Centrifugation	Filtration	Centrifugation
B_{max1} (%)	49 ± 7	35 ± 5	43 ± 5	41 ± 3
$\beta_{1\,obs}$ (min^{-1})	0.017 ± 0.001	0.023 ± 0.002	0.025 ± 0.007	0.023 ± 0.002
B_{max2} (%)	51 ± 7	65 ± 5	57 ± 5	57 ± 3
$\beta_{2\,obs}$ (min^{-1})	0.21 ± 0.02	0.67 ± 0.19	0.54 ± 0.18	0.74 ± 0.12

Dissociation constants and receptor densities.
Values are mean ± S.E.M. of three individual experiments run in triplicates (filtration) or duplicates (centrifugation).
Values were calculated from equations describing two exponential functions as described in Section 2.

Table 4
K_i values for different standard ligands in [^{3}H]ACPA rat membrane binding

	K_i (centrifugation) (μM)		K_i (filtration) (μM)	
	+KSCN	−KSCN	+KSCN	−KSCN
(*S*)-Glu	1.3 ± 0.2	1.2 ± 0.1	0.53 ± 0.15	0.69 ± 0.11
AMPA	0.077 ± 0.021[a]	0.22 ± 0.03	0.068 ± 0.014[c]	0.24 ± 0.01
ACPA	0.24 ± 0.02	0.19 ± 0.04	0.12 ± 0.01	0.093 ± 0.07
ATPA	9.5 ± 0.5	12 ± 0.7	8.0 ± 1.6	13 ± 7
KAIN	6.3 ± 0.8	6.1 ± 0.7	4.8 ± 0.8	6.1 ± 0.2
QUIS	0.081 ± 0.022	0.069 ± 0.024	0.027 ± 0.002[a]	0.048 ± 0.005
AMOA	42 ± 1[b]	21 ± 1	34 ± 11	33 ± 9
ATOA	190 ± 36[a]	70 ± 10	170 ± 13	160 ± 29
AMPO	50 ± 2[c]	11 ± 2	34 ± 3	19 ± 4
ATPO	48 ± 3[b]	6.0 ± 2.1	40 ± 5	14 ± 2
NBQX	0.097 ± 0.012	0.088 ± 0.021	0.15 ± 0.03	0.18 ± 0.01

K_i values for different standard ligands.
Displacement experiments and calculations were carried out as described in Section 2.
Experiments were carried out as centrifugation assays and filtration assays with and without KSCN.
[a], [b] and [c] indicates that a *t*-test proved differences in the pK_i values obtained in the presence and absence of KSCN, with a significance level of $P < 0.05$, $P < 0.01$, $P < 0.001$, respectively.
Values are mean ± S.E.M. of three individual experiments run in triplicates (filtration) or duplicates (centrifugation).
KAIN = Kainic acid; QUIS = Quisqualic acid.

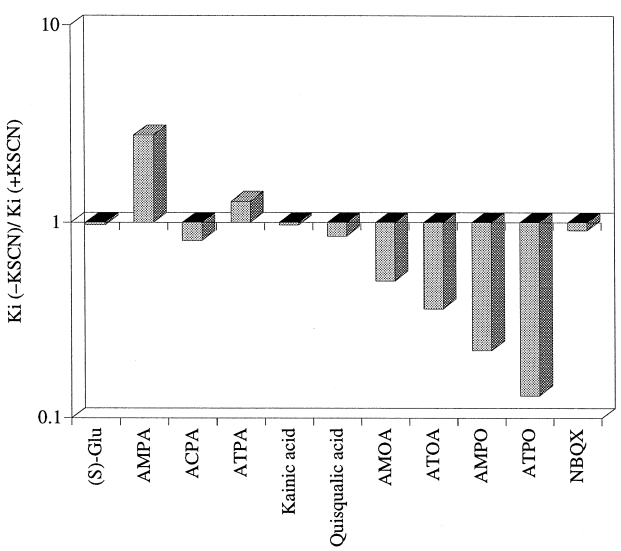

Fig. 7. Correlations between K_i-values determined in the presence and in the absence of KSCN, using centrifugation as the method to separate bound [^{3}H]ACPA from free [^{3}H]ACPA. Columns express the logarithmic relationship of $K_i(-\text{KSCN})/K_i(+\text{KSCN})$.

Table 5
K_D-values of [^{3}H]ACPA binding determined on cloned GluRs expressed in sf9 insect cells

	K_D (nM)
GluR1	45 ± 5
GluR2	15 ± 7
GluR3	28 ± 6
GluR4	20 ± 3
GluR5	330 ± 30

Values are mean ± S.E.M. of three individual experiments.

affinities of the antagonist ligands AMOA, ATOA, AMPO and ATPO showed the opposite effect of AMPA. Thus, the pK_i values decreased significantly in the absence of KSCN. Furthermore, the relative increase in affinity correlates with the potency of the antagonist determined in the cortical wedge model for the four antagonists: AMOA, being the weakest of the four antagonists in the cortical wedge preparation, shows a two-fold increase ($P < 0.01$ for centrifugation), whereas ATPO, being the most potent of the four antagonist, shows an eight-fold increase ($P < 0.01$ for centrifugation) in the absence of KSCN as compared to the values obtained in the presence of KSCN. The affinity of the antagonist NBQX was not affected by the addition of KSCN. The differences in K_i values were more evident in centrifugation assays as compared to filtration assays.

Hill coefficients (n_H) were determined for displacement curves for all ligands and were found to range from 0.6–1.0. For values significantly different from 1, equations describing two independent receptor populations were found not to fit the data better than equations describing one receptor population.

3.2. Binding studies on cloned iGluRs

[^{3}H]ACPA binding and K_D determination on cloned GluR1–4 expressed in sf9 insect cells showed, that [^{3}H]ACPA does not interact significantly different at any of the subunits. Affinities are listed in Table 5. [^{3}H]ACPA also showed binding to the kainic acid preferring subunit GluR5, but not GluR6, the affinity towards GluR5 being between seven to 22-fold weaker than that seen for GluR1–4.

3.3. Regional distribution of [^{3}H]ACPA binding

Quantitative receptor autoradiography studies comparing [^{3}H]AMPA, [^{3}H](*S*)-5-fluorowillardiine, and [^{3}H]ACPA binding in the presence or absence of KSCN, demonstrated that the three ligands, in the presence of KSCN, bind to the AMPA receptor with similar regional distribution (Table 6, Fig. 8). Highest densities were found in the hippocampus and the outer layers of cortex. Low densities were detected in the thalamic nuclei and the granula layer of the cerebellum. In the absence of KSCN, only very low levels of binding were detected for [^{3}H]AMPA, whereas the binding of [^{3}H](*S*)-5-fluorowillardiine and [^{3}H]ACPA was relatively insensitive to the presence of KSCN.

In order to determine whether levels of stimulation of binding by KSCN was different for the three ligands, the potentiation of binding by KSCN in the dentate gyrus and

Table 6
Regional distribution of specific binding of [^{3}H]ACPA, [^{3}H]AMPA, [^{3}H](*S*)-5-fluorowillardiine in rat brain, as determined by autoradiography

Region	[^{3}H]ACPA fmol/mg protein		[^{3}H]AMPA fmol/mg protein		[^{3}H](*S*)-5-Flu fmol/mg protein	
	− KSCN	+ KSCN	− KSCN	+ KSCN	− KSCN	+ KSCN
Cerebral cortex						
Subiculum	160 ± 9	190 ± 17	90 ± 12	330 ± 39	350 ± 20	580 ± 32
Enthorhinal cortex	104 ± 11	120 ± 14	59 ± 8	210 ± 38	180 ± 19	280 ± 24
Layer I–III	120 ± 8	160 ± 19	58 ± 9	230 ± 31	260 ± 20	330 ± 15
Layer IV–VI	81 ± 5	110 ± 11	45 ± 8	150 ± 19	210 ± 14	250 ± 16
Hippocampus						
CA1 stratum radiatum	230 ± 15	310 ± 17	97 ± 16	520 ± 39	570 ± 25	860 ± 34
Dentate gyrus	210 ± 17	290 ± 26	110 ± 17	480 ± 47	530 ± 34	760 ± 42
CA1 stratum pyramidale	210 ± 15	260 ± 16	73 ± 19	440 ± 39	460 ± 21	650 ± 39
CA1 stratum oriens	180 ± 14	210 ± 15	71 ± 14	320 ± 27	410 ± 24	660 ± 44
Hilus	162 ± 11	220 ± 17	85 ± 13	330 ± 40	370 ± 20	620 ± 39
CA3	140 ± 9	190 ± 16	69 ± 12	290 ± 34	300 ± 21	560 ± 36
Caudate putamen	80 ± 5	110 ± 12	43 ± 10	160 ± 16	180 ± 15	270 ± 10
Thalamus	47 ± 4	59 ± 8	32 ± 7	64 ± 12	75 ± 6	110 ± 7
Cerebellum						
Molecular layer	121 ± 10	180 ± 30	39 ± 11	150 ± 16	140 ± 15	320 ± 23
Granula layer	61 ± 34	57 ± 12	28 ± 7	65 ± 9	81 ± 7	120 ± 10

Values are mean ± S.E.M. in readings from six different rats.
Values are expressed as fmol/mg protein.
[^{3}H](*S*)-5-Flu = [^{3}H](*S*)-5-fluorowillardiine.

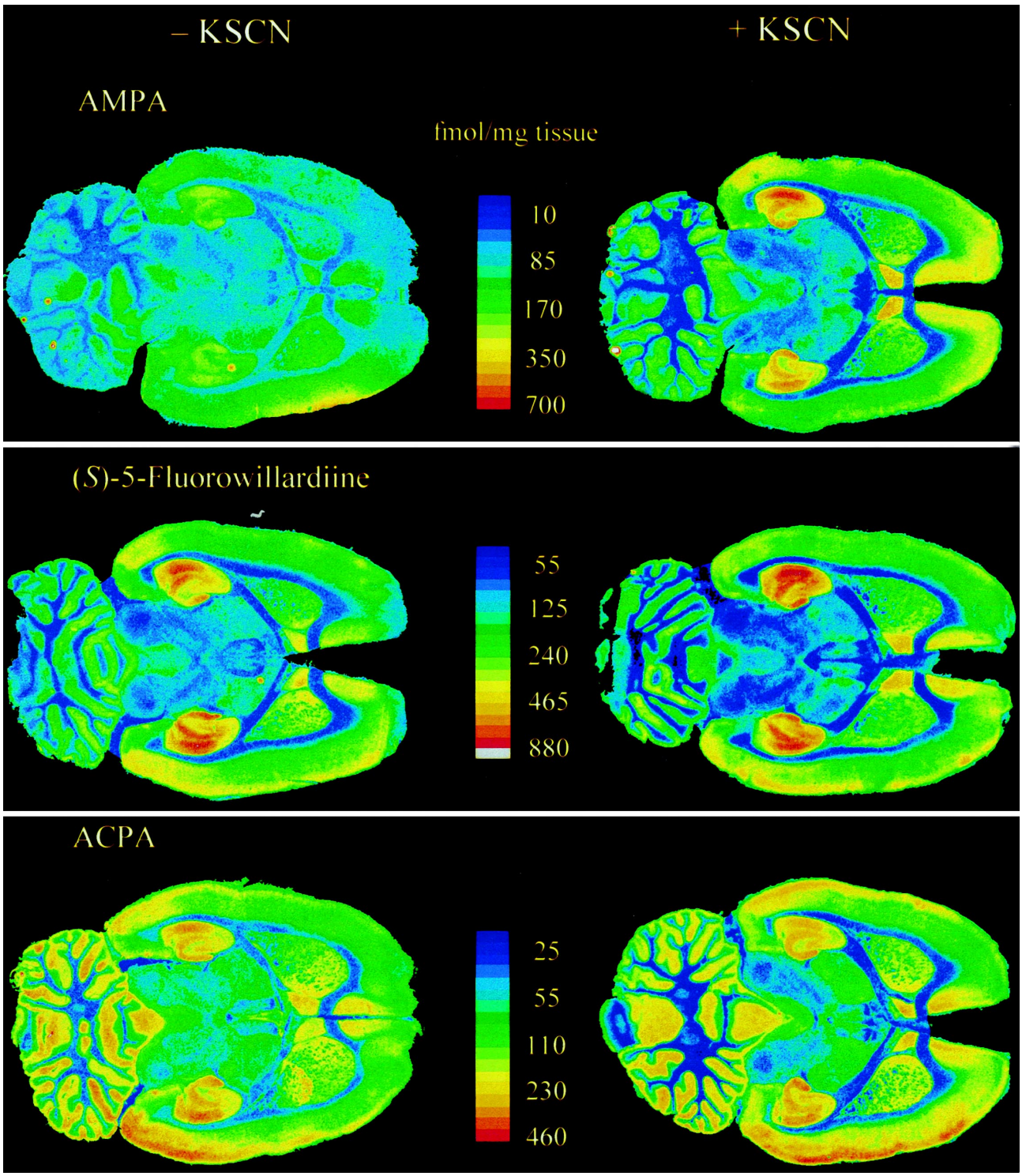

Fig. 8. Autoradiographic representation of the binding of 20 nM [^{3}H]AMPA (top), [^{3}H](*S*)-5-fluorowillardiine (middle), and [^{3}H]ACPA (bottom), respectively, in the presence and absence of 100 mM KSCN.

the molecular layer of the cerebellum was subjected to statistical analyses. *t*-Tests indicated that in both regions the binding of all three compounds was significantly increased by KSCN (cerebellum $P < 0.05$; dentate gyrus $P < 0.01$). The level of potentiation in the dentate gyrus, as compared to the molecular layer of the cerebellum, was similar for [^{3}H]AMPA (approximately 5 times) and [^{3}H]ACPA (approximately 1.4 times). On the other hand, [^{3}H](*S*)-5-fluorowillardiine was potentiated significantly more in cerebellum (2.2 times) than in the dentate gyrus (1.5 times) ($P < 0.01$) (Fig. 9). Comparison of the ratio of KSCN-induced potentiation between the ligands in the two

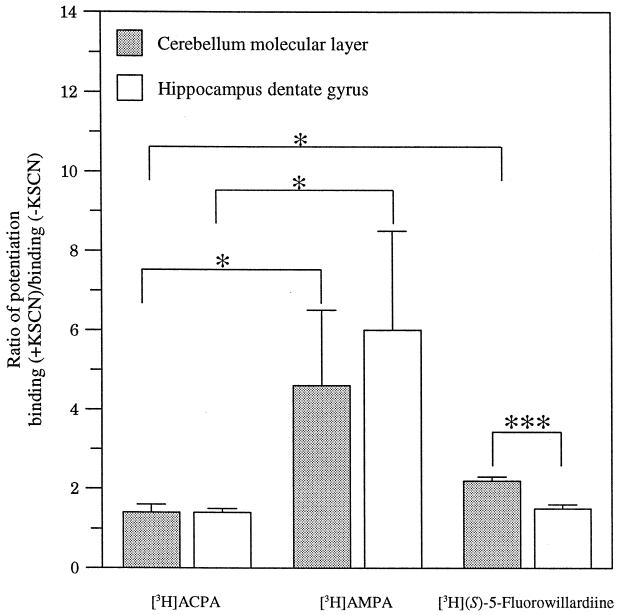

Fig. 9. KSCN potentiation of [^{3}H]ACPA, [^{3}H]AMPA and [^{3}H](*S*)-5-fluorowillardiine binding determined in autoradiographic studies in two different brain regions. * and *** indicates that *t*-test proved differences in the potentiation of the specific binding obtained in the presence and absence of KSCN, (as shown in Table 6), with significance levels of $P < 0.05$, $P < 0.001$, respectively.

regions showed that the binding of [^{3}H]ACPA was significantly less potentiated than [^{3}H]AMPA in both regions and significantly less than [^{3}H] (*S*)-5-fluorowillardiine in the dentate gyrus, whereas [^{3}H](*S*)-5-fluorowillardiine binding was significantly less potentiated than of [^{3}H]AMPA binding in the dentate gyrus.

4. Discussion

4.1. [^{3}H]ACPA binding characteristics

Rat membrane binding studies using [^{3}H]AMPA have previously shown that AMPA binds to two different binding sites with K_D values of 9 nM and 2440 nM, respectively (Honoré et al., 1982). In the presence of the chaotropic agent KSCN, the receptor density as well as the affinity for the low affinity binding site is increased substantially, the K_D values being 14 nM and 235 nM (Honoré and Drejer, 1988). We have now labelled the AMPA receptor agonist, ACPA, and saturation studies and scatchard analyses of filtration and centrifugation assays show that [^{3}H]ACPA binds to one binding site. Further investigations demonstrated that K_D values and the number of binding sites (B_{max}) obtained in the centrifugation assays were somewhat higher than those obtained when using filtration as the method of separation (Table 1). K_D values were two- to four-fold higher and B_{max} values were three- to four-fold higher as compared to the filtration assays, indicating that the binding of the ligand was not identical under these different experimental conditions. The higher density of [^{3}H]ACPA binding sites detected in centrifugation as compared to filtration may reflect that ACPA dissociates very rapidly from the binding sites. Thus, the additional seconds of wash in the filtration experiments will allow an extra amount of [^{3}H]ACPA to dissociate from its binding sites. As these binding sites will posses the lowest affinity for the [^{3}H]ACPA, the consequence is that the determined K_D value in filtration should be expected to be higher than in centrifugation. Although these binding studies failed to identify two distinct receptor populations, results suggest that under conditions that favour K_D-determination for low-affinity ligands (centrifugation) a higher proportion of a low affinity binding was present, thus giving higher K_D and B_{max} values. When using centrifugation as the method to separate bound ligand from free ligand, a smaller surface area is subjected to wash. This may result in a larger proportion of a low-affinity binding, thereby resulting in a higher K_D value and a higher density of binding sites. The differences in K_D and B_{max} values most probably reflect, that the affinity of the ligand is low, and as a result of this, a high proportion of binding sites are lost during the separation procedure. Alternatively, it may be hypothesized that a fraction of [^{3}H]ACPA binds to a low affinity conformation of the AMPA receptor with very low affinity, which in the present study has escaped identification both when using filtration and centrifugation as the method of separation. This surprisingly low receptor affinity determined for [^{3}H]ACPA using rat brain membranes could not be reproduced using cells expressing cloned GluR1–4, where low nanomolar receptor affinities were measured. In these latter binding experiments no selectivity was observed between the GluR1–4 subunits, and furthermore, [^{3}H]ACPA shows appreciable binding to the kainic acid subunit GluR5, thus showing lower selectivity towards AMPA receptor binding sites than AMPA.

In order to calculate the K_D values on the basis of kinetic studies, the association and dissociation constants were determined (Tables 1–3). The affinities calculated proved to be much higher, showing K_D values in the low nanomolar range, and thus did not correlate with the values obtained under saturation conditions. This lack of correlation has previously been reported for [^{3}H]AMPA binding (Honoré et al., 1982). An explanation to this could be, that the kinetically determined K_D value is based upon one of two binding sites (found in both association and dissociation experiments), whereas the saturated K_D value is based upon parameters from all of the [^{3}H]ACPA binding sites in the membrane preparation. Tables 2 and 3 indicates that the association rate (α_1) of [^{3}H]ACPA for a low affinity component is smaller than the corresponding dissociation (β_2), suggesting that the ligand dissociates faster than it associates. Taken together this clearly indicates that the mechanisms underlying the binding kinetics of [^{3}H]AMPA and [^{3}H]ACPA are far more complex than the assumed ‘one receptor site to one ligand molecule’ model

used to analyze the binding data. A further indication of this arises from the association experiments, where the data clearly suggested that [^{3}H]ACPA binds to two binding sites covering approximately 30% and 70%, respectively, of the total number of binding sites. The association of the 30% of the total receptor population is very fast, reaching equilibrium within the first minute, making a precise determination of this parameter difficult. Similarly, the dissociation of approximately 50% of the binding sites, found in the dissociation experiment is fast, making this parameter comparably difficult to establish.

Results of the association and dissociation studies were similar in the presence or absence of KSCN, as well as when using centrifugation or filtration as the method to separate bound ligand from free ligand.

4.2. The effect of the chaotropic agent KSCN

In contrast to what has been reported for [^{3}H]AMPA binding (Honoré and Drejer, 1988; Hawkins et al., 1995b; Hawkinson and Espitia, 1997), the K_D and B_{max} values for [^{3}H]ACPA were essentially the same in the presence and absence of KSCN, showing that the affinity of ACPA is not as sensitive to KSCN as that of AMPA. Similar results have been reported for the binding densities of [^{3}H](*S*)-5-fluorowillardiine, which were not altered by addition of KSCN (Hawkins et al., 1995a). These authors did, however, see an increase in the affinity of [^{3}H](*S*)-5-fluorowillardiine in the presence of KSCN, in contrast to the present findings for [^{3}H]ACPA. The mechanism of action of KSCN on the AMPA receptor in binding studies is not fully understood, however other groups have reported results comparable with the results obtained in the present study. It has been suggested that the effect of KSCN at the AMPA receptor is to induce a conformational change shifting the equilibrium to a more agonist-preferring conformation. This shift in conformation favors the binding of agonists like AMPA, thereby increasing the apparent potency and binding whereas compounds possessing equal affinity for the agonist and antagonist conformations, like CNQX and NBQX (Nielsen et al., 1988; Honoré et al., 1989), will retain the potency independently of the presence or absence of KSCN. Earlier studies by Ebert et al. (1994) have shown that the antagonists with structures resembling that of AMPA most likely are binding to a conformation of the AMPA receptor, which is not identical to receptor conformation with which the agonists like AMPA is interacting. The functional consequence of including KSCN into the media is therefore a reduced apparent affinity of antagonists structurally related to AMPA, whereas the agonists will increase in apparent potency. The affinity of AMPA towards [^{3}H]ACPA binding sites is increased three-fold ($P < 0.001$, *t*-test) in the presence of KSCN, but other AMPA receptor agonists tested did not seem to be equally sensitive to KSCN (Table 4 and Fig. 7). On the other hand, the affinities of the antagonists AMOA, ATOA, AMPO and ATPO for the [^{3}H]ACPA binding sites were increased significantly when KSCN was omitted (Table 4 and Fig. 7). The affinity of NBQX did not change significantly. Nielsen et al. (1995) have reported a minor increase in the affinity of NBQX in [^{3}H]AMPA binding in the absence of KSCN compared to assays including KSCN. The differences in affinity for the antagonists reported here with or without KSCN were more pronounced in the centrifugation assays. It has been shown that KSCN is able to antagonize AMPA responses in a noncompetitive manner, indicating an increased degree of desensitization of the receptor in the presence of KSCN (Bowie and Smart, 1993). Furthermore Wahl et al. (1996) have shown that ACPA-induced responses recorded from oocytes injected with rat brain mRNA encoding for subunit GluR1 flip, do not desensitize to the same extent as AMPA responses. These findings suggests that [^{3}H]ACPA, in contrast to [^{3}H]AMPA, binds to a nondesensitized state of the AMPA receptor. Since addition of KSCN reduces the affinity of the amino acid antagonists, structurally related to AMPA, in particular AMPO and ATPO containing phosphono groups, these antagonists seem to bind preferentially to the nondesensitized state of the AMPA receptor (Table 4). In contrast, this does not seem to be the case for the structurally unrelated antagonist NBQX.

4.3. Quantitative receptor autoradiography

Quantitative receptor autoradiographic studies with [^{3}H]ACPA, [^{3}H](*S*)-5-fluorowillardiine, and [^{3}H]AMPA showed, in agreement with other studies, highest densities of AMPA binding sites in the hippocampus and the outer layers of the cortex. Lowest densities were found in the thalamic nuclei and in the granula layer of the cerebellum. The binding of radioligand in the molecular layer of the cerebellum was found to be approximately 60%, 35%, and 35% for [^{3}H]ACPA, [^{3}H](*S*)-5-fluorowillardiine, and [^{3}H]AMPA, respectively, relative to the binding of radioligand in the dentate gyrus, indicating that [^{3}H]ACPA binds to a greater extent in the cerebellum (Table 6). The sensitivity of these [^{3}H]AMPA binding sites towards stimulation with KSCN was similar to that observed in the dentate gyrus of the hippocampus for [^{3}H]ACPA, whereas the binding of [^{3}H](*S*)-5-fluorowillardiine was potentiated more in the cerebellum as compared to the dentate gyrus ($P < 0.001$). The degree of potentiation was different for the three ligands, being: 5, 1.4 and 2 for [^{3}H]AMPA, [^{3}H]ACPA and [^{3}H](*S*)-5-fluorowillardiine, respectively. In agreement with the homogenate binding studies (Table 1), these data therefore strongly suggests that [^{3}H]ACPA preferentially binds to a non-KSCN-inducible receptor conformation, whereas [^{3}H]AMPA appears to have the highest affinity for the KSCN-inducible high-affinity AMPA receptor conformation.

In summary, [^{3}H]ACPA was found to bind to a single receptor population under the conditions described. This receptor population was relatively insensitive to modula-

tion by KSCN both regarding K_D and B_{max} values. Kinetic studies showed that there was no significant difference in association and dissociation in the absence or presence of KSCN. In addition, similar results were obtained when centrifugation or filtration was used as the method to separate bound from free [^{3}H]ACPA. Kinetics studies, on the other hand, did indicate that two distinct receptor populations might be present, but these data did not correlate with the data obtained in the saturation experiments. Displacement studies revealed that addition of KSCN changed the affinity of a series of antagonists for the AMPA receptor site, the antagonists having higher affinities in the absence of KSCN. Autoradiographic studies supported the result from the homogenate binding, and indicated that [^{3}H]ACPA binds to the cerebellum to a greater extent than [^{3}H]AMPA and [^{3}H](*S*)-5-fluorowillardiine. Since ACPA, AMPA and (*S*)-5-fluorowillardiine seem to bind to and activate AMPA receptors in a dissimilar fashion, these three agonists may form a battery of useful tools for studies of AMPA receptor mechanisms. Obviously, any future agonist pharmacophore model of the AMPA receptor must be developed under consideration of the structural and pharmacological differences of these three agonists.

Acknowledgements

This work was supported by grants from the Danish State Biotechnology Program (1991–1995) and the Lundbeck Foundation.

References

Begtrup, M., Sløk, F.A., 1993. Equilibrium control in bromomethylation: an expedient route to 2-amino-3-(3-hydroxy-5-methylisoxazol-4-yl)propionic acid (AMPA). Synthesis 9, 861–863.

Bennett, J.P.J., Yamamura, H.I., 1985. Neurotransmitter, hormone, or drug receptor binding methods. In: Yamamura, H.I., Enna, S.J., Kuhar, M.J. (Eds.), Neurotransmitter Receptor Binding. Raven Press, New York, NY, pp. 61–89.

Bowie, D., Smart, T.G., 1993. Thiocyanate ions selectively antagonize AMPA-evoked responses in *Xenopus laevis* microinjected with rat brain mRNA. Br. J. Pharmacol. 109, 779–787.

Cheng, Y., Prusoff, W.H., 1973. Relationship between the inhibition constant (K_i) and the concentration of inhibitor which causes 50 percent inhibition (IC_{50}) of an enzymatic reaction. Biochem. Pharmacol. 22, 3099–3108.

Collingridge, G., Watkins, J.C., 1994. The NMDA Receptor. Oxford Univ. Press, Oxford.

Ebert, B., Madsen, U., Lund, T.M., Lenz, S.M., Krogsgaard-Larsen, P., 1994. Molecular pharmacology of the AMPA agonist, (*S*)-2-amino-3-(3-hydroxy-5-phenyl-4-isoxazolyl)propionic acid [(*S*)-APPA] and the AMPA antagonist, (*R*)-APPA. Neurochem. Int. 24, 507–515.

Hawkins, L.M., Beaver, K.M., Jane, D.E., Taylor, P.M., Sunter, D.C., Roberts, P.J., 1995a. Characterization of the pharmacology and regional distribution of (*S*)-[^{3}H]-5-fluorowillardiine binding in rat brain. Br. J. Pharmacol. 116, 2033–2039.

Hawkins, L.M., Beaver, K.M., Jane, D.E., Taylor, P.M., Sunter, D.C., Roberts, P.J., 1995b. Binding of a new radioligand (*S*)-[^{3}H]AMPA to rat brain synaptic membranes: effects of a series of structural analogues of the non-NMDA receptor agonist willardiine. Neuropharmacology 34, 405–410.

Hawkinson, J.E., Espitia, S.A., 1997. Effects of thiocyanate and AMPA receptor ligands on (*S*)-5-fluorowillardiine, (*S*)-AMPA, and (*RS*)-AMPA binding. Eur. J. Pharmacol. 329, 213–221.

Honoré, T., Drejer, J., 1988. Chaotropic ions affect the conformations of quisqualate receptors in rat cortical membranes. J. Neurochem. 51, 457–461.

Honoré, T., Lauridsen, J., Krogsgaard-Larsen, P., 1982. The binding of [^{3}H]AMPA, a structural analog of glutamic acid, to rat brain membranes. J. Neurochem. 38, 173–178.

Honoré, T., Drejer, J., Nielsen, E.Ø., Nielsen, M., 1989. Non-NMDA glutamate receptor antagonist ^{3}H-CNQX binds with equal affinity to two agonist states of quisqualate receptors. Biochem. Pharmacol. 38, 3207–3212.

Krogsgaard-Larsen, P., Hansen, J.J., 1992. Excitatory Amino Acid Receptors: Design of Agonists and Antagonists. Ellis Horwood, Chichester.

Krogsgaard-Larsen, P., Ferkany, J.W., Nielsen, E.Ø, Madsen, U., Ebert, B., Johansen, J.S., Diemer, N.H., Bruhn, T., Beattie, D.T., Curtis, D.R., 1992. Novel class of amino acid antagonists at non-*N*-methyl-D-aspartic acid excitatory amino acid receptors. Synthesis, in vitro and in vivo pharmacology and neuroprotection. J. Med. Chem. 34, 123–130.

Lauridsen, J., Honoré, T., Krogsgaard-Larsen, P., 1985. Ibotenic acid analogues. Synthesis, molecular flexibility, and in vitro activity of agonists and antagonists at central glutamic acid receptors. J. Med. Chem. 28, 668–672.

Leatherbarrow, R.J., 1992. GraFit version 3.0. Erithacus Software, Staines, UK.

Madsen, U., Wong, E.H.F., 1992. Heterocyclic excitatory amino acids. Synthesis and biological activity of novel analogues of AMPA. J. Med. Chem. 35, 107–111.

Madsen, U., Bang-Andersen, B., Brehm, L., Christensen, I.T., Ebert, B., Kristoffersen, I.T.S., Lang, Y., Krogsgaard-Larsen, P., 1996. Synthesis and pharmacology of highly selective carboxy and phosphono isoxazole amino acid AMPA receptor antagonists. J. Med. Chem. 39, 1682–1691.

Monaghan, D.T., Wenthold, R.J., 1997. The Ionotropic Glutamate Receptors. Humana Press, Totowa, NJ.

Morgan, R.C., Mercer, L.D., Cincotta, M., Beart, P.M., 1991. Binding of [^{3}H]AMPA to nonchaotrope, non-detergent treated rat synaptic membranes: characteristics and lack of effect of barbiturates. Neurochem. Int. 18, 75–84.

Nielsen, E.Ø., Cha, J.-H.J., Honoré, T., Penney, J.B., Young, A.B., 1988. Thiocyanate stabilizes AMPA binding to the quisqualate receptor. Eur. J. Pharmacol. 157, 197–203.

Nielsen, E.Ø, Johansen, T.H., Wätjen, F., Drejer, J., 1995. Characterization of the binding of [^{3}H]NS 257, a novel competitive AMPA receptor antagonist, to rat brain membranes and brain sections. J. Neurochem. 65, 1264–1273.

Wahl, P., Madsen, U., Banke, T., Krogsgaard-Larsen, P., Schousboe, A., 1996. Different characteristics of AMPA receptor agonists acting at AMPA receptors expressed in *Xenopus* oocytes. Eur. J. Pharmacol. 308, 211–218.

Wheal, H.V., Thomson, A.M., 1995. Excitatory Amino Acids and Synaptic Transmission. Academic Press, London.